Identification and characterization of NVP-BEZ235, a new orally available dual phosphatidylinositol 3-kinase/mammalian target of rapamycin inhibitor with potent *in vivo* antitumor activity

Sauveur-Michel Maira,[1] Frédéric Stauffer,[1] Josef Brueggen,[1] Pascal Furet,[1] Christian Schnell,[1] Christine Fritsch,[1] Saskia Brachmann,[1] Patrick Chène,[1] Alain De Pover,[1] Kevin Schoemaker,[3] Doriano Fabbro,[2] Daniela Gabriel,[2] Marjo Simonen,[2] Leon Murphy,[4] Peter Finan,[4] William Sellers,[5] and Carlos García-Echeverría[1]

[1]Oncology Disease Area and [2]Center for Proteomic Chemistry, Novartis Institutes for Biomedical Research, Novartis Pharma AG, Basel, Switzerland; [3]Novartis Vaccines and Diagnostics, Inc., Emeryville, California; and [4]Developmental and Molecular Pathways and [5]Oncology Disease Area, Novartis Institutes for Biomedical Research, Cambridge, Massachusetts

Abstract

The phosphatidylinositol 3-kinase (PI3K)/Akt/mammalian target of rapamycin inhibitor (mTOR) pathway is often constitutively activated in human tumor cells, providing unique opportunities for anticancer therapeutic intervention. NVP-BEZ235 is an imidazo[4,5-*c*]quinoline derivative that inhibits PI3K and mTOR kinase activity by binding to the ATP-binding cleft of these enzymes. In cellular settings using human tumor cell lines, this molecule is able to effectively and specifically block the dysfunctional activation of the PI3K pathway, inducing G_1 arrest. The cellular activity of NVP-BEZ235 translates well in *in vivo* models of human cancer. Thus, the compound was well tolerated, displayed disease stasis when administered orally, and enhanced the efficacy of other anticancer agents when used in *in vivo* combination studies. *Ex vivo* pharmacokinetic/pharmacodynamic analyses of tumor tissues showed a time-dependent correlation between compound concentration and PI3K/Akt pathway inhibition. Collectively, the preclinical data show that NVP-BEZ235 is a potent dual PI3K/mTOR modulator with favorable pharmaceutical properties. NVP-BEZ235 is currently in phase I clinical trials. [Mol Cancer Ther 2008;7(7):1851–63]

Introduction

Phosphatidylinositol 3-kinase (PI3K) and its downstream effector Akt are frequently deregulated in human cancers (1). To be fully active, Akt needs to be phosphorylated on two critical residues: Thr^{308} (T308-Akt) and Ser^{473} (S473-Akt). The upstream kinase responsible for the T308 site phosphorylation is PDK1. The identity of the kinase responsible for the S473 phosphorylation (PDK2) has been a matter of debate as many candidates, including Akt itself, ILK, PDK1, or DNA protein kinase (DNA-PK), have been proposed (2). Compelling evidence have emerged recently that indicate that the rapamycin-insensitive mammalian target of rapamycin inhibitor mTORC2 complex (mTOR in complex with rictor, Sin1, and mLst8) is PDK2 (3–7).

Once activated, Akt phosphorylates several substrates involved in various cellular processes including cell growth, proliferation, survival, and metabolism (8). All of these cellular processes are being considered as crucial features for the establishment and the maintenance of the tumorigenic phenotype (9). Overactivation of the PI3K pathway could be the result of different genetic alterations (10). First, systemic sequencing of the PIK3CA gene has revealed the presence of somatic mutations (11), occurring along the coding region of the gene but with most of them present in two hotspots. The first one is located in the helical domain (with a preponderance for the E545K mutation), and the second one in the kinase domain (with a preponderance for the H1047R mutation). When overexpressed, the corresponding mutant proteins have been found to be oncogenic *in vitro* and *in vivo* (12–14). Genetic ablation of the PI3K mutant allele in the colorectal cancer cell lines HCT116 and DLD-1 reduced their oncogenic properties (15).

Second, the PI3K antagonistic dual protein/lipid phosphatase PTEN has been found inactivated or deleted in a large fraction of advanced human cancer, including glioblastoma, endometrial, breast, thyroid, prostate cancer, and melanoma. PTEN-inactivated tumor cells exhibit elevated Akt kinase activity due to uncontrolled phosphorylation of T308 and S473. Under some circumstances, the Ras oncogene or activated receptor tyrosine kinases have also been shown to mediate their transforming potential through aberrant PI3K signaling (16). Regardless of the mechanism, the prevalence of PI3K/Akt signaling abnormalities in human tumors suggests an important role for

Received 1/8/08; revised 3/6/08; accepted 4/3/08.

The costs of publication of this article were defrayed in part by the payment of page charges. This article must therefore be hereby marked *advertisement* in accordance with 18 U.S.C. Section 1734 solely to indicate this fact.

Requests for reprints: Sauveur-Michel Maira, Oncology Disease Area, Novartis Institutes for Biomedical Research, Novartis Pharma AG, CH4002 Basel, Switzerland. Phone: 41-61-69-67910; Fax: 41-61-69-65571. E-mail: sauveur-michel.maira@novartis.com

doi:10.1158/1535-7163.MCT-08-0017

this pathway in cancer pathogenesis and furthermore provides strong support for the development of targeted therapeutic anticancer application of agents that inhibit the activation of the PI3K/Akt pathway.

To date, modulators of the PI3K family have only provided proof-of-concept in preclinical settings. The first-generation PI3K inhibitors include the viridin soil bacteria product wortmannin (17) and LY294002, a morpholino-derivative of quercetin (18). Although suffering from unfavorable pharmaceutical properties, toxicity, and crossover inhibition of other lipid and protein kinases (19), they have been extensively used as tool compounds against a variety human tumor histotypes *in vivo* and showed the potential utility of PI3K inhibitors as cancer therapeutics (20–22).

In an initial medicinal chemistry effort to develop PDK1 inhibitors using the imidazo-quinoline scaffold, lead compounds were found to also inhibit class I PI3K (23). Further optimization for class I PI3K inhibition using a structure-based design approach led to the identification of NVP-BEZ235, a dual pan-class I PI3K and mTOR kinase inhibitor. We report herein the biochemical and cellular characterization of NVP-BEZ235, showing its potency and selectivity for efficient PI3K pathway blockade. Finally, its antitumor activity in experimental cancer models, including *in vivo* PK/PD tumor tissue correlations, is reported.

Materials and Methods

Chemical Compounds

NVP-BEZ235 was synthesized in the Global Discovery Chemistry Group (Novartis Pharma, Novartis Institutes for Biomedical Research Oncology) and provided as a 10 mmol/L stock solution in 100% DMSO. Working solutions were prepared freshly before addition to the cell media. Final DMSO concentration was kept constant at 0.1% in control and compound-treated cells. Wortmannin and LY294002 were from Alexis Biochemicals.

In vitro Protein Kinase, PI3K, and mTOR Assays

All the biochemical *in vitro* protein kinase assays shown in Table 1 were already described (24). PI3Kα, β, and δ proteins were composed of the iSH2 domain of p85 NH_2-terminally fused to the full-length protein p110 protein, with the exception of α that also did not contain the last 20 amino acids. PI3Kγ was produced as full-length protein deleted for its first 144 amino acids (25). All constructs were fused to a COOH-terminal His tag for convenient purification and then cloned into the pBlue-Bac4.5 (for α, β, and δ isoforms) or pVL1393 (for γ isoform) plasmids. The different vectors were then cotransfected with BaculoGold WT genomic DNA using methods recommended by the vendor for production of the respective recombinant baculoviruses and proteins. Compounds were tested for their activity against PI3K using a Kinase-Glo assay (26). The kinase reaction was done in 384-well black plate (Corning). Each well was loaded with 50 nL of test items (in 90% DMSO) and 5 μL reaction buffer [10 mmol/L Tris-HCl (pH 7.5), 50 mmol/L NaCl, 3 mmol/L $MgCl_2$, 1 mmol/L DTT, and 0.05% CHAPS] containing 10 μg/mL PI substrate (L-α-phosphatidylinositol; Avanti Polar Lipids; prepared in 3% octyl-glucoside) and the PI3K proteins (10, 25, 10, and 150 nmol/L of p110α, p110β, p110δ, and p110γ, respectively) were then added. The reaction was started by the addition of 5 μL of 1 μmol/L ATP prepared in the reaction buffer and ran for either 60 (for p110α, p110β, and p110δ) or 120 min (for p110γ) and subsequently terminated by the addition of 10 μL Kinase-Glo buffer (Promega). The plates were then read in a Synergy 2 reader (BioTek) for luminescence detection.

Cell Lines and Cell Culture

The highly metastatic human prostate tumor cell line PC3M was obtained from Dr. J. Fiedler (M. D. Anderson Cancer Center). The U87MG glioblastoma tumor line was obtained from Dr. Adrian Merlo (University of Basel). The TSC1-null MEF cell line was obtained from Dr. David Kwiatkowski (Brigham and Women's Hospital). The

Table 1. Biochemical profile of NVP-BEZ235 against selected protein kinases and class I PI3Ks

	Enzyme	IC_{50} (nmol/L)	Enzyme	IC_{50} (nmol/L)
Class I PI3K	p110α	4 ± 2 (n = 3)	p110β	75 ± 45 (n = 3)
	p110α-H1047R	4.6 ± 0.8 (n = 3)	p110δ	7 ± 6 (n = 3)
	p110α-E545K	5.7 ± 1.0 (n = 3)	p110γ	5 ± 4 (n = 3)
Protein kinases	VEGFR1/Flt1	>10,000 (n = 3)	Fak	>10,000 (n = 3)
	Flt3	>10,000 (n = 3)	Jak2	>10,000/9,000
	HER1/ErbB1	>10,000/8,500	c-Abl	>10,000 (n = 3)
	IGFI-R	>10,000 (n = 2)	c-Src	>10,000 (n = 3)
	EphB4	>10,000 (n = 3)	PKA	>10,000 (n = 3)
	Ret	>10,000 (n = 3)	Akt1/PKBα	>10,000 (n = 3)
	Tie-2/Tek	>10,000 (n = 3)	PDK1	>10,000 (n = 2)
	c-Met	>10,000 (n = 3)	V599E-B-Raf	>10,000 (n = 3)
	K650E-FGFR	>10,000 (n = 3)	CDK1	>10,000 (n = 3)

NOTE: *In vitro* kinase assays were done with the indicated recombinant PI3K lipid or protein kinases in the presence of increasing concentrations of NVP-BEZ235 as described in Materials and Methods. The concentration responsible of 50% inhibition of the activity (IC_{50}) is reported as average ± 1 SD (nmol/L).

colorectal HCT116 and HT29 cell lines and the breast cancer cell line were purchased from the American Type Cell Collection (CCL-247, HTB-38, and HTB-20, respectively). The NIH-3T3 derived NWT21 cell line that stably expresses the insulin-like growth factor-I receptor (IGF-IR) was described elsewhere (24). All the cell lines were cultured at 37°C in a 5% CO_2 and 80% relative humidity atmosphere incubator in high-glucose DMEM (Life Technologies) complemented with 10% fetal bovine serum, 2 mmol/L glutamine, 1% penicillin-streptomycin, and 1% sodium pyruvate. U2OS-FKHRL1 cells were obtained by infecting with the FKHRL1-GFP retrovirus (details on the cloning strategy and map of the vector are available on request). Stable expressers were obtained after serial dilution of G418-resistant pools of cells.

Cell Lysate Preparation, Immunoblotting, and Antibodies

For biochemical characterization, 2×10^6 cells were seeded per 10 cm dish. After 18 h, the medium was discarded and replaced with 10 mL fresh medium containing the test items. Unless specified in the figure legend, the incubation period was 30 min. For agonist activation, cells were first starved for 18 h in 9 mL medium containing only 0.05% fetal bovine serum. Then cells were pretreated for 30 min with 1 mL medium containing the test items and subsequently simulated for 10 min with the various agonists (final concentrations: 50 ng/mL IGF-I, Prepro-Tech; 60 ng/mL interleukin-4 Sigma; 1 mmol/L anisomycin, Alomone Labs) for a period of 10 min. Cells were washed twice, lysed, and processed as described by Western blot analysis as described. The primary antibodies used were as follows: anti-S473P-Akt, anti-T308P-Akt, anti-S9P-GSK3β, anti-T389P-$p70^{S6K}$, anti-YP/TP-extracellular signal-regulated kinase 1/2, anti-YP/TP-p38, anti-YP/TP-c-Jun NH_2-terminal kinase 1/2, anti-Y751P-platelet-derived growth factor receptor, anti-$p21^{Cip1/waf1}$, anti-$p27^{kip1}$, and anti-Ser^{15}-p53 antibodies were from Cell Signaling Technologies; anti-Akt, anti-T32P-FKHRL1, and anti–platelet-derived growth factor receptor antibodies were from Upstate; anti-IGF-IR and anti–epidermal growth factor receptor antibodies were from Santa Cruz; anti-GSK3α/β, anti-Y641P-Stat6, anti-S1981P-ATM, anti-T2609 DNA-PKcs, and anti-Y1316P-IGF-IR were from Bio-Source International, Becton Dickinson, Rockland, GenTex, and internal production, respectively.

S473P-Akt, T308P-Akt, and pS6RP Levels Quantification

T308P-Akt and S473P-Akt ELISA Assays. U87MG cells (4×10^4) were platted in 96-well culture plates and incubated for 18 h. In parallel, ELISA test plates (Becton Dickinson) were prepared with the anti-Akt coating antibody (Santa Cruz). Medium in plates was discarded and replaced by medium containing the test items (eight concentrations in triplicate). After 30 min, cells were rinsed and immediately lysed. Cell extracts (50 μL) were then transferred into ELISA plates and incubated for 3 h at 4°C. After three washes, 50 μL secondary antibody (anti-S473P-Akt, CST, or the anti-T308P-Akt; Santa Cruz) was added and plates were incubated for 16 h at 4°C. Finally, the horseradish peroxidase–conjugated antibody (Sigma) was added for 2 h and the immune complexes assayed with 100 μL substrate (Pierce). The luminescence was read on a Top-Count NXT (Packard Bioscience) luminometer, and the IC_{50} was determined with the XL-Fit module for Microsoft Excel (IDBS software).

S235/236P-RPS6 in Cell Western Assay. TSC1-null MEF cells (1×10^4) were seeded in 96-well black plates (Greiner Bio-one). After 24 h, cells were treated for 1 h with the test items and directly fixed by addition of 100 μL of 3.7% formaldehyde. Cells were washed four times with 100 μL/well PBS containing 0.1% Triton X-100 for 4 min and blocked with 50 μL/well Odyssey blocking buffer (Li-COR Biosciences) for 2 h at room temperature with gentle agitation. The anti-Ser^{235}/Ser^{236}-RPS6 antibody (CST) was then incubated overnight at room temperature with gentle agitation. After five washes, the cells were stained with an IRDye 800 antibody (Rockland). After an additional washing step, DNA staining was done with TO-PRO-3 iodide (Invitrogen). The phospho-S6 signals were then measured in triplicates using a Li-COR Odyssey Infrared Imager.

Forkhead Translocation Assay

For the translocation assay, 5×10^3 U2OS-GFP-FKHRL1-expressing cells were seeded and incubated for 24 h in 96-well Packard View plates. Cells were then starved for 24 h and the medium was replaced with fresh medium containing the test items. After 1 h, cells are fixed with a prewarmed formaldehyde solution (3.7% in PBS). After three washes with PBS, nuclei are stained with Hoechst dye (Sigma). The fluorescence was imaged and pictures were taken with a Zeiss Axiovert 100 inverted epifluorescence microscope.

Establishment of Xenograft Tumors, Efficacy Studies, Compound Preparation, and Analytics

Establishment of tumors, group randomization, tumor, and body weight recording during efficacy studies were described elsewhere (24). All experimental procedures (approved by the Kantonales Veterinäramt Basel-Stadt under license 1769) strictly adhered to the Eidgenössisches Tierschutzgesetz and the Eidgenössische Tierschutzverordnung. Antitumor activity is expressed as %T/C (mean increase of tumor volumes of treated animals divided by the mean increase of tumor volumes of control animals multiplied by 100) and/or as tumor regression (%Reg) calculated as [(mean tumor volume at the start of treatment - mean tumor volume) / (mean tumor volume at the start of treatment)] × 100. Data are presented as mean ± 1 SE. Comparisons between groups and vehicle control group were done using either one-way ANOVA or ANOVA on ranks followed by Dunnett's tests when data were respectively either normally distributed or not. For all tests, the level of significance was set at $P < 0.05$. Calculations were done using SigmaStat version 2.03 (Jandel Scientific). NVP-BEZ235 (free base) was formulated in NMP/polyethylene glycol 300 (10/90, v/v). Solutions (5 mg/mL) were prepared fresh each day of dosing as

follows: the powder was dissolved in NMP on sonication, and the remaining volume of polyethylene glycol 300 was added. The application volume was 10 mL/kg. For analytics, frozen tissues were minced and then homogenized in an equal volume of ice-cold PBS (Sigma) using a Polytron homogenizer (IKA). After acetonitrile precipitation and centrifugation, supernatants were analyzed by reverse-phase high-performance liquid chromatography/UV on a Merck-Hitachi/LaChrom equipment including a Nucleosil 100-5 C18 column. Samples were then eluted with a linear gradient of 10% to 90% (v/v) acetonitrile in water containing 0.05% (v/v) trifluoroacetic acid over a period of 20 min at a flow rate of 1 mL/min. The compounds were detected by UV absorbance at 340 nm, and concentrations were determined by the external standard method using peak heights.

Results

NVP-BEZ235 Potently Inhibits PI3K in an ATP Competitive Manner

The imidazo[4,5-*c*]quinoline scaffold is able to mimic the H-bond interactions of the adenine moiety of ATP with the hinge region using several binding modes (23). This unique feature makes this chemical template an attractive starting point for a structure-based drug design effort, particularly for targets in which some level of structural information is available. The reported X-ray structure of the kinase domain of p110γ (25, 27) and a previously identified dual PDK1/PI3K inhibitor were used as the basis for the design of imidazo[4,5-*c*]quinoline derivatives with PI3K but not PDK1 inhibitory properties. Medicinal chemistry efforts to optimize drug-like and pharmacologic properties led to the synthesis and identification of NVP-BEZ235 (Fig. 1A).

NVP-BEZ235 was tested against class I PI3K using an ATP depletion (Kinase-Glo) assay (Table 1). Although the compound shows slightly lower activity against the β paralogue (IC_{50}, 75 nmol/L), it can be considered a pan-class I PI3K inhibitor. The compound was also found to be as active against the E545K or H1047R mutant forms of PI3Kα and to poorly inhibit (IC_{50} >5 μmol/L) a representative panel of protein kinases, including the PI3K effectors Akt and PDK1 (Table 1). Confirming the low nanomolar potency obtained on PI3Kα, NVP-BEZ235 displayed a 2-log left-shifted inhibition curves when compared with LY294002 (IC_{50}, 2.2 and 4.7 versus 745 and 813 nmol/L, respectively) in two different and additional PI3K biochemical assays (ADP release and MaxiSorp assays, respectively) using full-length p85α/p110α protein complex (Supplementary Fig. S1).[6]

Figure 1B shows NVP-BEZ235 docked in a PI3Kγ-based three-dimensional homology model of the kinase domain of PI3Kα, a model that is in agreement with the recently determined PI3Kα three-dimensional structure (28). It is proposed that the compound binds in the ATP-binding cleft of the lipid kinase using three H-bond interactions. The nitrogen atom of the core quinoline ring is involved in a key H-bond interaction with the backbone of the conserved PI3Kα Val^{851} (Val^{882} in γ). This canonical interaction with the hinge region is observed for ATP and for all the PI3K-inhibitors for which X-ray cocrystal structures exist (25). The second and third H-bond interactions (*dotted lines*) involve the backbone of the conserved Asp^{933} (Asp^{964} in PI3Kγ) and the side chain of the conserved Ser^{774} (Ser^{806} in PI3Kγ). These H-bond interactions are complemented by favorable van der Waals contacts with conserved hydrophobic residues of the ATP catalytic site, including Met^{772} (Met^{804} in PI3Kγ), Tyr^{836} (Tyr^{837} in PI3Kγ), and Met^{922} (Tyr^{953} in PI3Kγ). When tested in presence of increasing ATP concentrations (26 nmol/L to 400 μmol/L; Fig. 1C), the IC_{50} values for NVP-BEZ235 and LY294002 toward PI3Kα inhibition increased in a linear manner, in agreement with an inhibition by ATP competition.

NVP-BEZ235 Specifically Blocks the PI3K Pathway in Cells

The cellular activity of the compound was assessed using tumor cell lines with a hyperactivated PI3K pathway. When exposed to the U87MG glioblastoma PTEN-negative cell line, NVP-BEZ235 reduced S473P-Akt (Fig. 2A, *top*) and T308P-Akt (*middle*) levels in a dose-dependent manner. A similar pattern of inhibition was observed using the PTEN-null PC3M prostate tumor cell line (Supplementary Fig. S2).[6] No effects on total Akt protein levels were observed showing that the compound has no effect on protein stability. Quantification of S473-Akt and T308P-Akt levels by ELISA revealed that 50% reduction occurred at a compound concentration of 8.0 ± 3.2 nmol/L (n = 6) and 30 ± 15 nmol/L (n = 31), respectively. Pulse-chase experiments revealed a rapid recovery to basal S473P-Akt level (Fig. 2A, *bottom*), on compound removal from the medium, showing that the inhibitory activity is reversible.

To determine whether the specificity against PI3K observed in the biochemical profiling translates into cellular settings, the effects of the compound on survival (IGF-I), mitogenic (platelet-derived growth factor and epidermal growth factor), stress (anisomycin), cytokine (interleukin-4) and DNA damage (doxorubicin) regulated signaling pathways were evaluated. At a concentration of 250 nmol/L, NVP-BEZ235 was able to reduce IGF-I-induced S473P-Akt levels below the limit of detection, whereas the phosphorylation of the p85 binding site on IGF-IR (Y1316) was not altered (Fig. 2B). Similar results were obtained with the PI3K inhibitors LY294002 and wortmannin. As expected, RAD001 (mTOR inhibitor) and STI571 (Bcr-Abl inhibitor) were not affecting IGF-I-induced phosphorylation of Akt on Ser^{473}. Moreover, IGF-I-induced activation of the mitogen-activated protein kinase pathway was not altered on treatment with NVP-BEZ235. Similar results were obtained when cells were stimulated with the epidermal growth factor or platelet-derived growth factor (data not shown). Hence, it seems unlikely that

[6] Supplementary material for this article is available at Molecular Cancer Therapeutics Online (http://mct.aacrjournals.org/).

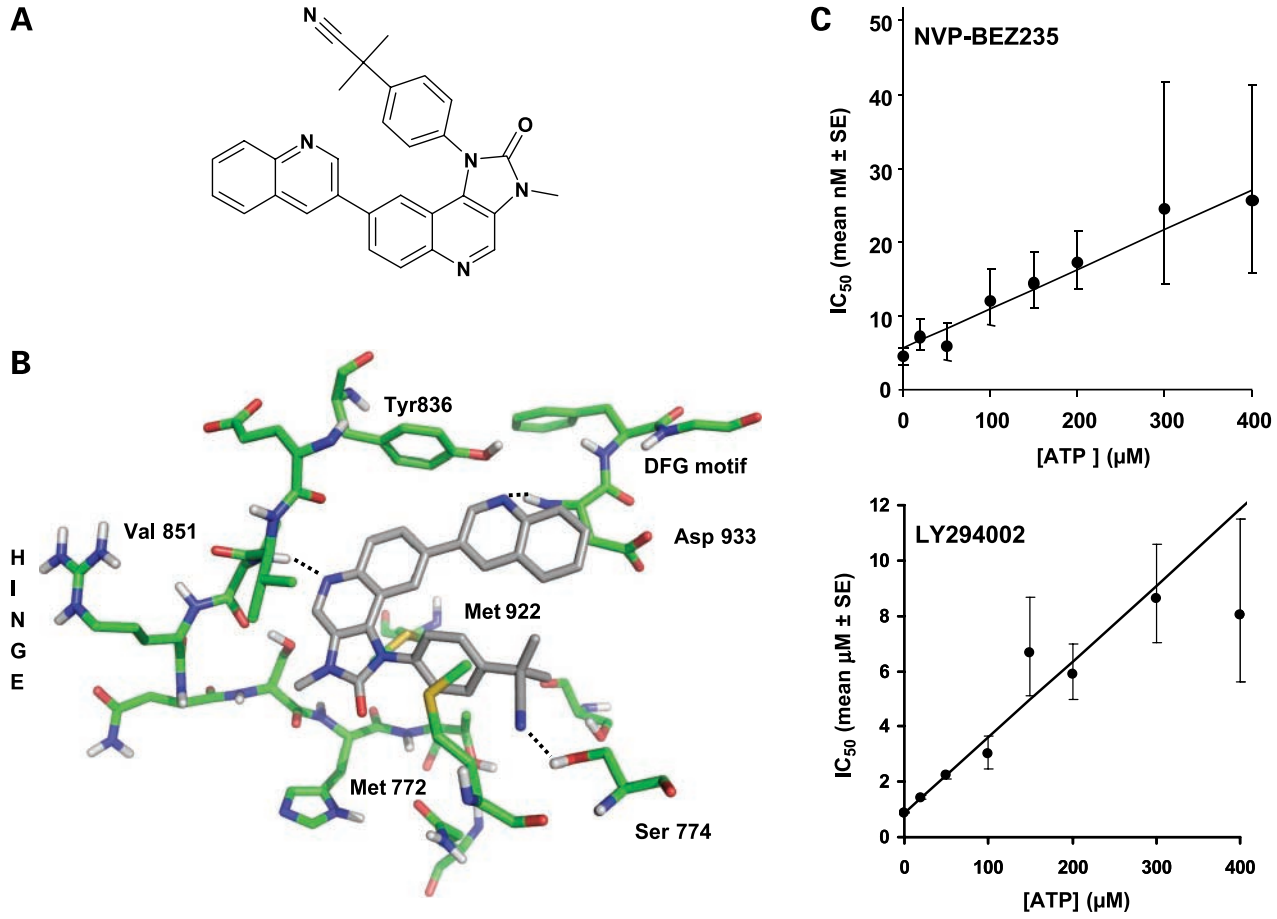

Figure 1. Enzymatic characterization of NVP-BEZ235. **A,** structure of NVP-BEZ235. **B,** binding mode of NVP-BEZ235 docked in the catalytic site of PI3Kα. The model was generated using the coordinates of known PI3Kγ crystal structures, particularly those of the complex with staurosporine (PDB code 1E8Z), based on a standard sequence alignment. This binding mode hypothesis was the result of systematic docking (followed by energy minimization) of the compound in the ATP cleft. All possible orientations were considered to determine which one was the most consistent with the available structure-activity relationship, particularly with regard to the importance of the H-bond acceptor nitrogen atoms present in the chemical structure of the inhibitor for high potency. **C,** NVP-BEZ235 is an ATP competitive inhibitor. IC_{50} values determined using the MaxiSorp assay were plotted against the ATP concentrations used in the presence of either NVP-BEZ235 or LY294002. The large error bars at high ATP concentrations are due to isotopic dilution (lower counts). Data were fitted by linear curve fitting with weights ($1 / SE^2$). The positive slope of the straight line indicates a competitive effect ($P < 0.01$) for both inhibitors. Note that this analysis does not exclude the presence of a noncompetitive component (mixed inhibition).

NVP-BEZ235 inhibits PI3K pathway activation by interfering with the kinase activity of the evaluated receptor tyrosine kinases. At a concentration of 250 nmol/L, NVP-BEZ235 did not inhibit anisomycin-induced phosphorylation of c-Jun NH_2-terminal kinase and p38 in NWT-21, U87MG, and A549 cells (Fig. 2C). Thus, under the tested experimental conditions, NVP-BEZ235 did not influence the activity of the c-Jun NH_2-terminal kinase/p38 stress pathway components such as the mitogen-activated protein kinase kinase (MKK4 and MKK3/6, respectively), mitogen-activated protein kinase kinase kinase (MEKK1/4 and MLK3/6, respectively), and small GTPases such as Rac and Cdc42 (29). Whereas 250 nmol/L NVP-BEZ235 efficiently blocked interleukin-4-induced S473P-Akt levels, activated Stat6 phospholevels were not affected on treatment, excluding an effect of the compounds on Jak kinases at this concentration (Fig. 2D).

Due to the lack of suitable biochemical assays for ATM or DNA-PK, the activities of NVP-BEZ235 against these enzymes were evaluated using cellular readouts. ATM and DNA-PK are involved in the DNA damage repair machinery. DNA strand breaks induced by DNA-damaging agents potently activate ATM and cause its autophosphorylation (30). ATM and DNA-PK can then phosphorylate downstream effectors like p53 (31). When exposed for 24 h to the topoisomerase II inhibitor doxorubucin, U87MG cells displayed a robust increase in S1981P-ATM autophosphorylation and S15P-p53 levels (Fig. 2E, *top*). Cotreatment with NVP-BEZ235 had no effect on neither DNA double-strand break–induced ATM activation nor p53 activation. In contrast, under the same experimental conditions, S473P-Akt levels were strongly reduced. The effect on doxorubicin induced on S1981P-ATM or T2609P-DNA-PK autophosphorylation levels were investigated in parallel at

NVP-BEZ235 concentrations of 250 and 1,250 nmol/L (Fig. 2E, *bottom*). Although the S1981P-ATM autophosphorylation levels were poorly affected at any of the dose tested, only the highest one caused a significant reduction of the T2609P-DNA-PK levels. Hence, these data show that in the range of concentrations of NVP-BEZ235 that significantly affect PI3K signaling (250 nmol/L), the compound does not inhibit ATM or DNA-PK, two protein kinases with a PI3K catalytic domain highly homologous to class IA PI3K.

Effects of NVP-BEZ235 on Akt Downstream Effectors and mTOR

Reduced phosphorylation of Akt on treatment with NVP-BEZ235 (250 nmol/L) or the internal reference compounds such as wortmannin (250 nmol/L) or LY294002 (20 μmol/L;

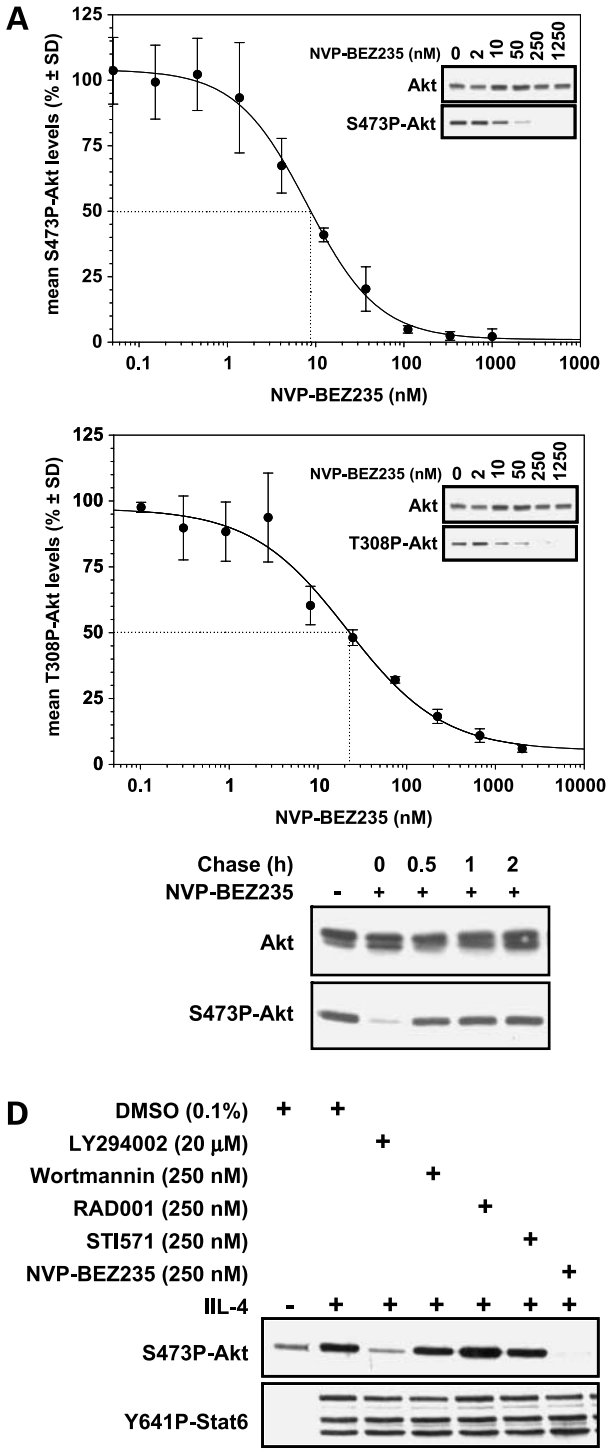

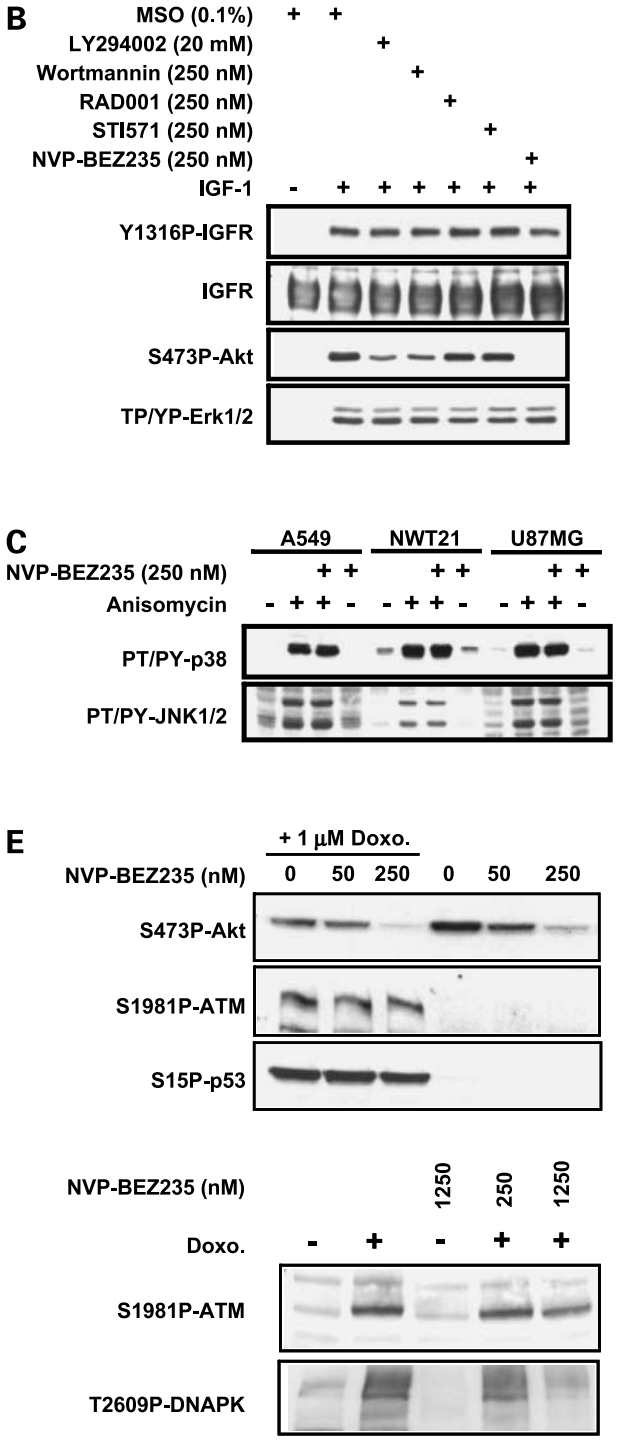

ref. 32) correlated with the inhibition of Akt downstream effectors, such as GSK3β and FKHRL1 (FOXO3a; Fig. 3A). In agreement with the Akt-dependent but mTORC1-independent regulation of forkhead factors, no effect on FKHRL1 localization was observed with the allosteric mTOR inhibitor RAD001 (33). Consistent with these results, treatment of U2OS cells with NVP-BEZ235 stably expressing a GFP-FKHRL1 chimeric protein with NVP-BEZ235 led to its complete nuclear relocalization as shown by the time-dependent increased in the fluorescent signal obtained in the nuclei (Fig. 3B). A similar effect was observed when cells were treated with LY294002, but not with RAD001 or DMSO, for which most of the fluorescence emission remained cytosolic. Complete nuclear translocation was achieved between 9 and 12 min after NVP-BEZ235 addition (Supplementary Fig. S3A).[6] NVP-BEZ235 treatment of U2OS-GFP-FKHRL1 cells transiently transfected with a luciferase reporter gene controlled by a forkhead binding elements (34) caused significant and dose-dependent transcriptional activity (50% maximum induction for 76 nmol/L, $n = 2$; Supplementary Fig. S3B),[6] showing that once relocalized to the nucleus FKHRL1 can bind DNA and activate transcription.

NVP-BEZ235 significantly reduced the phosphorylation levels of the mTOR activated kinase $p70^{S6K}$ (Fig. 3A). This kinase is activated by the TORC1 complex, which itself is relieved from a negative regulation by the TSC1/2 complex in a PI3K- and Akt-dependent manner (35). Cell line lacking functional TSC complexes (TSC1-null MEF) are characterized by a constitutively active mTORC1 complex (36). As expected, TSC1-null MEF exposed RAD001 showed a complete reduction of S235/S236P-RPS6 levels, even at the lowest concentration tested (1 nmol/L). Under similar experimental conditions, NVP-BEZ235 also led to a reduction of S235/S236P-RPS6 levels with an IC_{50} of 6.5 nmol/L (Fig. 3C), suggesting that NVP-BEZ235 can directly inhibit the mTOR kinase, as the kinase domain of mTOR is highly homologous to the one of class IA PI3K. The activity of NVP-BEZ235 against mTOR was confirmed using a biochemical mTOR K-LISA assay (IC_{50}, 20.7 nmol/L; Supplementary Fig. S4A).[6] To test whether NVP-BEZ235 inhibits both mTORC1 and mTORC2 complexes, immunokinase assays were done using 4E-BP1 (Phas) as a substrate. Maximum activity of TAP-tagged immunoprecipitated Raptor (mTORC1) or Rictor (mTORC2) kinase complexes was reached after an incubation period of 30 min (Supplementary Fig. S4B).[6] The addition of NVP-BEZ235 to otherwise similar assay conditions caused a concentration-dependent decrease in mTORC1 and mTORC2 activities (Fig. 3D). Altogether, these data show that NVP-BEZ235 is also a mTORC1/2 catalytic inhibitor.

NVP-BEZ235 Possesses Strong Antiproliferative Activity

Both PTEN-null cell lines PC3M and U87MG showed a dose-dependent reduction in cell proliferation when treated with increasing concentrations of NVP-BEZ235, with an average GI_{50} of 10 to 12 nmol/L. However, no obvious decline in cell viability was observed on treatment with NVP-BEZ235, as the compound was never able to reduce the cell number below the amount originally plated (corresponding to the 0% plateau; Fig. 4A). Cell cycle content analysis of growing PC3M cells revealed that the G_1 population increased from 66.4% (DMSO controls) to 74.1% and 92.3% on treatment of the cells with 10 to 50 nmol/L NVP-BEZ235, respectively (Fig. 4B). A similar effect was observed when the cells were treated with LY294002. For both compounds, no clear sub-G_1 population could be detected, indicating a limited ability of both inhibitors for cell death induction in this cell line. NVP-BEZ235 incubation significantly increased the amount of the cyclin-dependent kinase inhibitor $p27^{Kip1}$ in the p53-negative PC3M cell line. Accordingly, p53-regulated gene product levels in basal or treated (DNA-damaging cisplatin agent, LY294002 or NVP-BEZ235) conditions were not detectable in this cell line. A similar study was therefore done in the p53-positive cell line HCT116. As expected, cisplatin but not LY294002 or NVP-BEZ235 treatments increased $p21^{Cip1/Waf1}$ levels, showing that PI3K inhibition does not influence $p21^{Cip1/Waf1}$ protein levels.

NVP-BEZ235 Is an Orally Available PI3K Inhibitor with Well-Tolerated Antitumor Activity

The pharmacokinetic properties of NVP-BEZ235 were originally evaluated in PC3M tumor-bearing nude mice. At a dose of 50 mg/kg, NVP-BEZ235 appeared rapidly in plasma with a C_{max} of 1.68 μmol/L at 0.5 h and a C_{24h} of

Figure 2. Cellular profiling of NVP-BEZ235. **A,** dose-dependent and reversibility effects on activated Akt levels. U87MG cells were incubated with increasing amounts of NVP-BEZ235 for 30 min. Cells were then lysed and cell extracts were analyzed either by ELISA or Western blotting (inlets) to assess total or S473P (*top*) or T308P-Akt levels (*middle*). Alternately, after 30-min exposure (250 nmol/L), cells were washed and incubated in fresh medium without compound for the indicated period. Cells were then lysed and analyzed by Western blotting either for Akt or S473P-Akt levels (*bottom*). **B,** effects on the IGF-I signaling pathway. NWT21 cells were starved, preincubated for 60 min with the indicated compounds for 30 min, and stimulated for 10 min with IGF-I. Cells were then lysed and cell extracts were analyzed by Western blotting for the indicated protein levels. **C,** effects on the stress regulated mitogen-activated protein kinase pathways. The indicated cell lines were preincubated with NVP-BEZ235 and subsequently challenged with the stress agent anisomycin for 15 min. Cells were then lysed and cell extracts were analyzed by Western blotting for activated c-Jun NH_2-terminal kinase and p38 levels. **D,** effects on the Jak-Stat pathway. HT-29 cells were starved for 18 h, preincubated for 60 min with the indicated inhibitors, and subsequently stimulated with interleukin-4 for 15 min. Cells were then lysed and cell extracts were analyzed by Western blotting for activated Akt and Stat-6 levels. **E,** effects on the ATM and DNA-PK-DNA repair regulated pathways. U87MG cells were incubated with doxorubicin either with 50 and 250 nmol/L (*top*) or 250 and 1,250 nmol/L (*bottom*) of NVP-BEZ235 or the vehicle control (control) for a period of 24 h. Cells were then lysed and cell extracts were analyzed by Western blotting for activated S473P-Akt, S15P-p53, and S1981P-ATM levels (*top*) or S1981P-ATM and T2609P-DNA-PK levels (*bottom*). Note that the time exposure of 24 h does not allow a direct comparison with the data obtained in **A**, in which the cells were kept in contact with the compound for a period of 30 min.

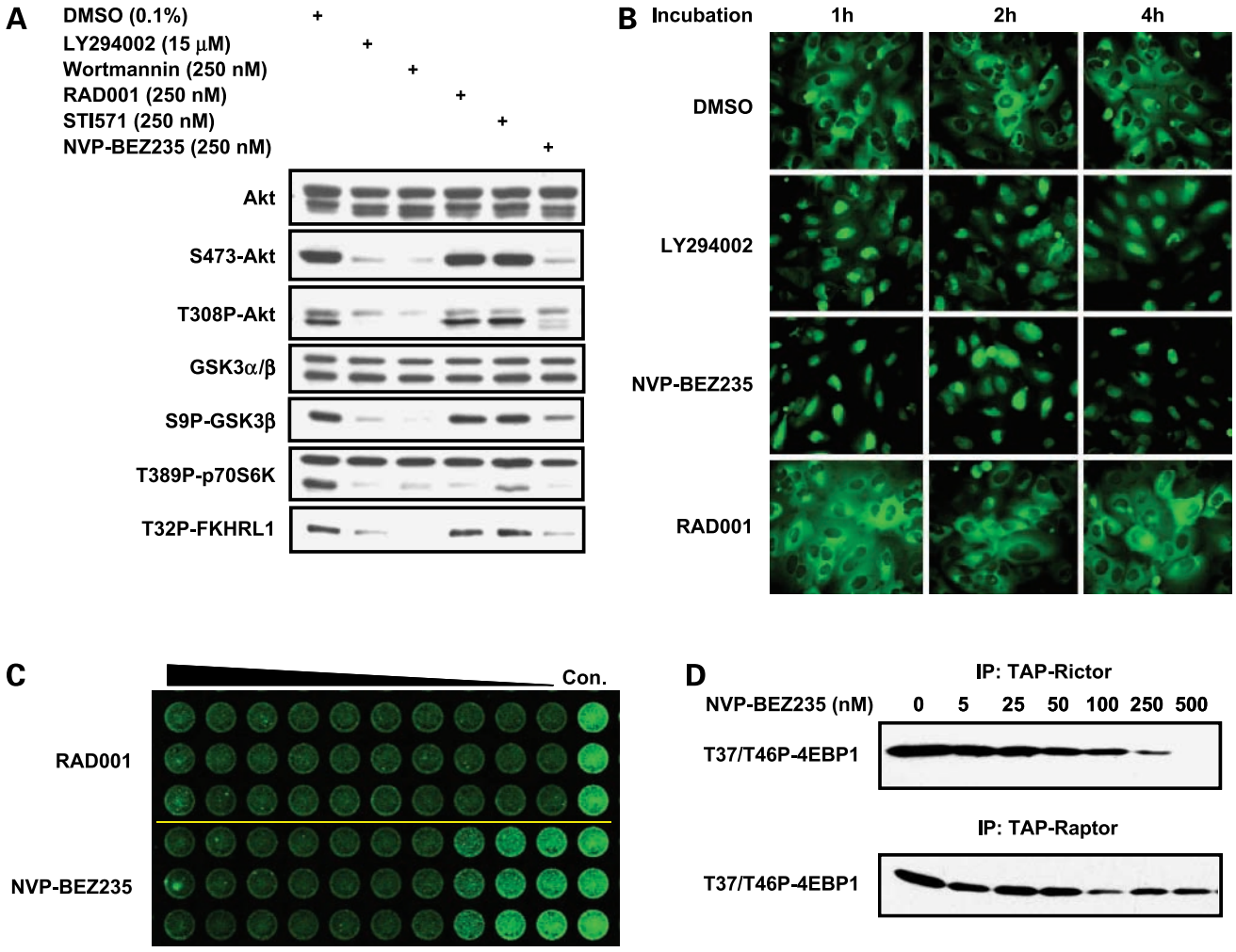

Figure 3. Effects of NVP-BEZ235 on Akt downstream effectors and mTOR. **A,** U87MG cells were treated with the indicated inhibitors for 30 min. Cells were then lysed and cell extracts were analyzed by Western blotting for phosphorylated Akt (both sites), GSK3β, $p70^{S6K}$, and FKHRL1 (FOXO3A). **B,** effect of LY294002 (10 μmol/L), NVP-BEZ235 (250 nmol/L), or RAD001 (250 nmol/L) on FKHRL1-GFP translocation. U2OS-GFP-FOXO3A cells were incubated for either 1, 2, or 4 h with the compounds and then fixed and the nuclei were stained with Hoechst. The cells were imaged with a standard inverted epifluorescence microscope. **C,** NVP-BEZ235 inhibits mTORC1 activity in cells. TSC1-null MEF cells were incubated with increasing doses of either RAD001 or NVP-BEZ235 for 1 h. Cells were then fixed, blocked, and stained with the anti-phospho-S6 (Ser^{235}/Ser^{236}). **D,** NVP-BEZ235 inhibits mTORC1 and mTORC2. IgG-Sepharose pull-downs of HeLa cells stably expressing either TAP-tagged Rictor (500 μg) or TAP-tagged Raptor (30 μg) were subjected to *in vitro* kinase assays with 4EBP1 (Phas) as a substrate for 30 min (TAP-Rictor) or 20 min (TAP-Raptor) at 30°C with increasing amounts of NVP-BEZ235. Kinase reactions were analyzed by Western blotting to assess inhibition on Ser^{37}/Ser^{46} phosphorylation of 4EBP1.

0.03 μmol/L. In the tumor tissue, the C_{max} attained was 2.05 nmol/g at 1 h (T_{max}), which decreased to 0.23 nmol/g after 24 h (Fig. 5A). NVP-BEZ235 is eliminated relatively quickly from the liver. *In vivo* analysis of the S473P-Akt levels in the tumor tissue revealed that maximum inhibition was obtained 1 h after dosing (corresponding to the tumor C_{max}), and persistent inhibition was observed still 16 h after treatment, with almost complete recovery to basal levels obtained in two of four tumors at 24 h after dose (Fig. 5B). Pharmacokinetic simulation based on this study revealed that steady-state levels would be achieved between 3 and 5 days, when dosing either at 50 mg/kg given daily or at 25 mg/kg given twice daily. Differences between the dosage regimens would reside in the predicted tumor peak levels (2.6 versus 1.6 nmol/g, respectively) whereas through levels would remain almost comparable (0.53 versus 0.60 μmol/L, respectively). Taking into consideration this pharmacokinetic simulation, chronic treatment of PC3M tumor-bearing animals was done at 25 mg/kg p.o. NVP-BEZ235 twice daily. Using this schedule, a statistically significant inhibition of tumor growth was observed, with a final T/C value of 22% after 10 days of treatment (Fig. 5C). The treatment was well tolerated as concluded from the nonstatistically significant effect of NVP-BEZ235 on body weight gain (Fig. 5C) and by the fact that none of the animals died during the course of the study. The antitumor effect was well correlated with the inhibition of S473P-Akt in the tumor tissue 1 or 18 h after

the last dose detected either by Western blotting of tumor extracts or by immunostaining of tumor sections (Fig. 5D). Compound concentrations at these time points were 1.32 nmol/g at 1 h and 0.51 nmol/g at 18 h, close to the predicted values for steady-state peak levels (see above).

Activation of the PI3K pathway through loss of PTEN function in glioblastoma multiforme has been correlated with resistance to epidermal growth factor receptor–targeted therapies (37), radiotherapy, and alkylating agents such as temozolomide (38). It is therefore anticipated that PI3K inhibitors might be beneficial in the treatment of this malignancy. To assess the antitumor activity of NVP-BEZ235 against a PTEN-null glioblastoma multiforme tumor model, s.c. U87MG tumor-bearing animals were treated either with NVP-BEZ235 alone or in combination with the standard of care temozolomide (39). As a single agent, a dose-dependent effect on tumor growth was observed when animals were treated with suboptimal (25 mg/kg/d once per day) to optimal (45 mg/kg/d once per day) doses of NVP-BEZ235 (Fig. 6A), with almost tumor stasis achieved at the highest dose tested (T/C of 22%, 18%, and 5.5%, at 25, 35, and 45 mg/kg, respectively). No body weight loss was observed during the course of the experiment in all groups (Fig. 6A). The antitumor activity was in this model also well correlated with reduction in S473P-Akt levels in the tumor (Fig. 6B). Because the activation of PI3K pathway is linked to survival, PI3K inhibitors would be ideal candidates for combination therapies. Temozolomide introduces O^6-methylguanine adducts in DNA, which mispairs with thymine during the next cell cycle of replication, leading to G_2 checkpoint activation and subsequent cell death. Akt activation was shown to bypass the G_2 arrest on temozolomide treatment (40), suggesting that Akt inactivation might positively influence temozolomide effects. Treatment of U87MG tumor-bearing animals with temozolomide alone resulted in efficient block of tumor growth (T/C of 5.2%), whereas the addition of NVP-BEZ235 even caused regression of the tumors (69%) without statistically significant effect on body weight gain (Fig. 6C). Altogether, these preliminary *in vivo* efficacy results suggest that NVP-BEZ235 causes disease stasis when administered orally as a single agent and can enhance the efficacy of other anticancer agents when used in *in vivo* combination studies.

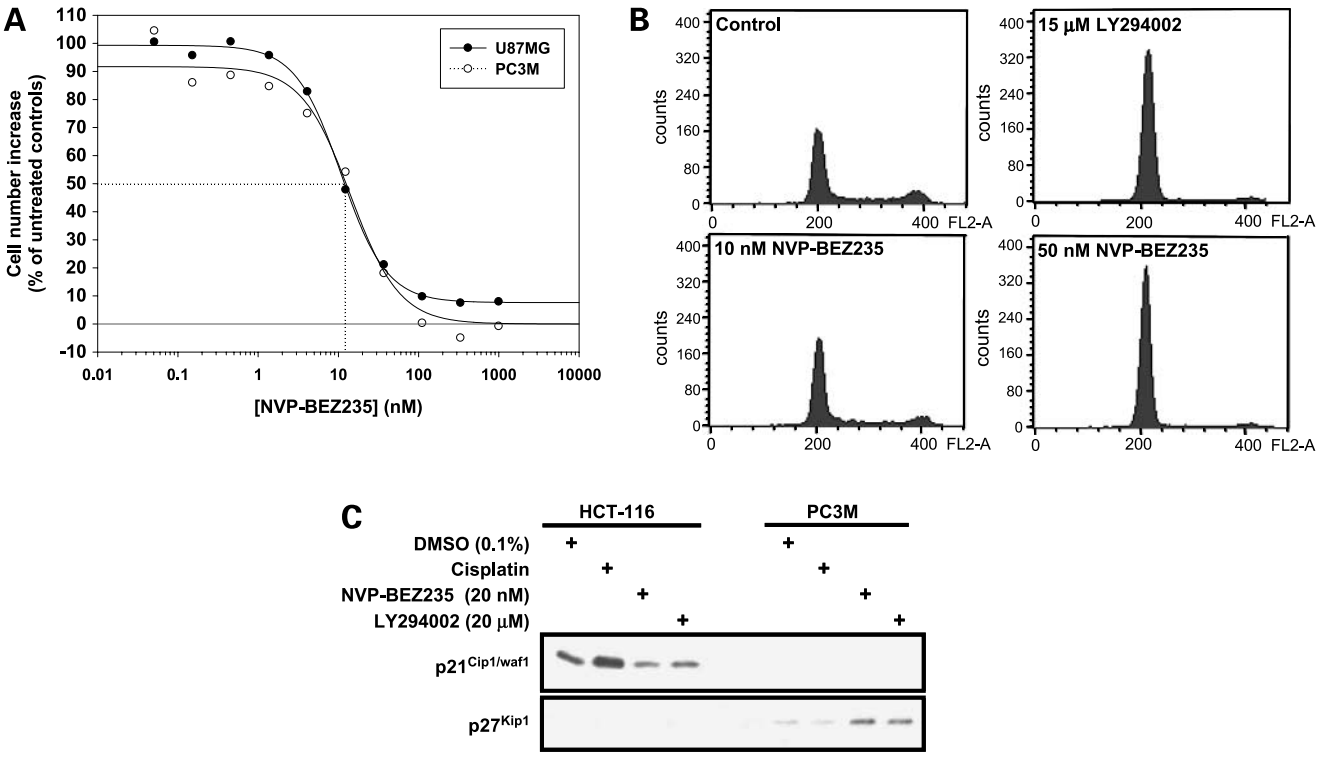

Figure 4. Effects of NVP-BEZ235 on proliferation and the cell cycle. **A,** U87MG and PC3M cells were incubated with increasing amount of NVP-BEZ235 for 72 h. Viable cells were then stained and cell proliferation was estimated with a standard methylene blue staining assay. Cell proliferation is expressed as a percentage of the average difference in cell number observed in NVP-BEZ235-treated cells divided by the average difference observed in untreated controls (100% represents the maximum cell proliferation observed and 0% represents the inoculums; the number of cells at the time in which the compound is added to the medium). **B,** PC3M cells were incubated with the indicated compound for 24 h. Determination of cell number was then determined by fluorescence-activated cell sorting. **C,** PC3M and HCT116 cells were incubated for 24 h with the indicated compounds. Cells were then lysed and cell extracts were analyzed by Western blotting for $p21^{Cip1/Waf1}$ and $p27^{Kip1}$ cyclin-dependent kinase inhibitors.

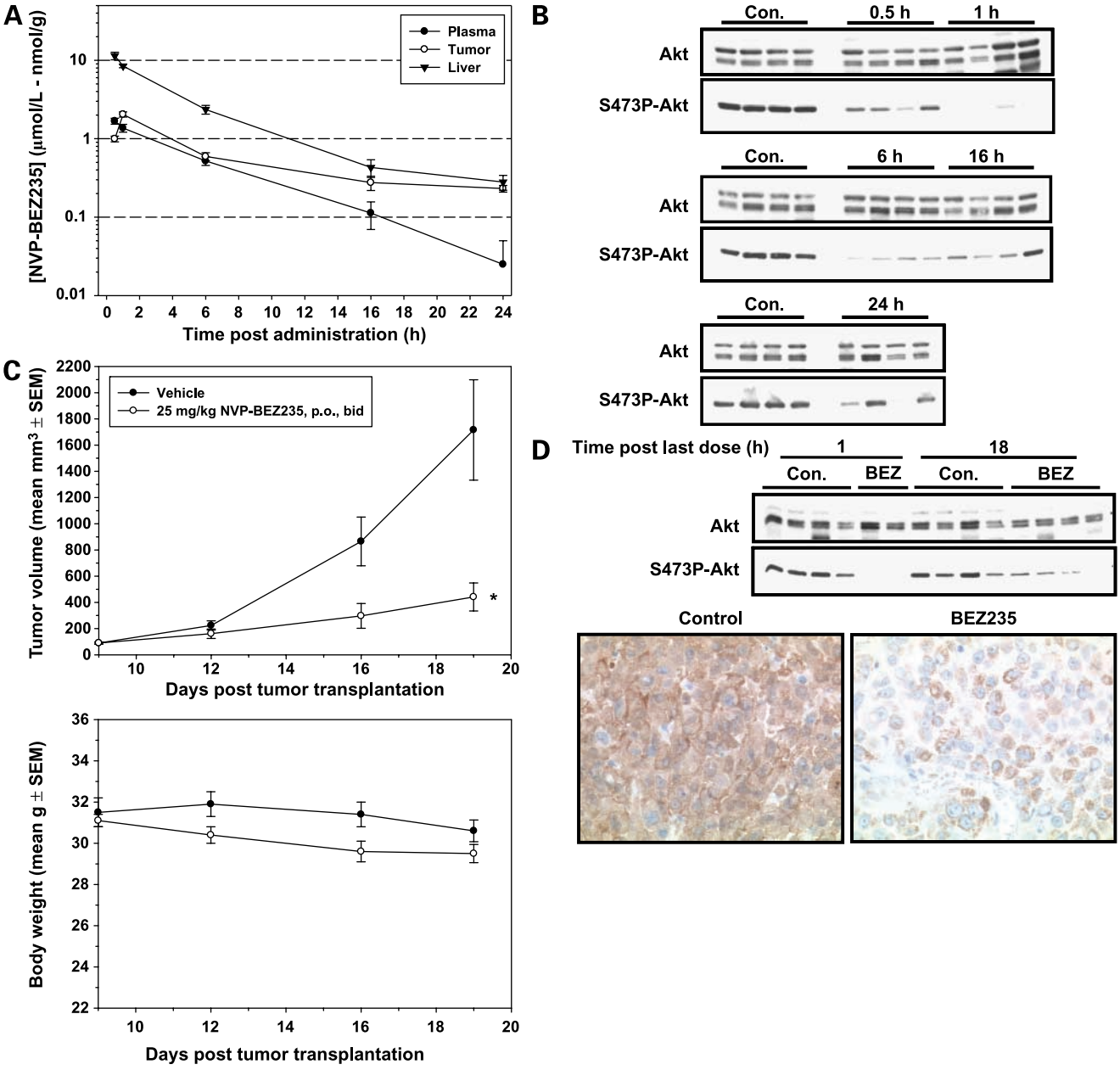

Figure 5. Pharmacokinetic/pharmacodynamic relationship in tumor-bearing animals. **A** and **B,** PC3M tumor-bearing animals ($n = 4$) were treated orally with 50 mg/kg NVP-BEZ235, and animals were sacrificed 1, 2, 6, 16, and 24 h after dosing. Compound concentration in plasma, liver, and tumor (**A**) was determined by high-performance liquid chromatography/UV (sensitivity, 0.1 μmol/L). In parallel, tumor extracts were used to determine activated Akt levels determined by Western blotting (**B**). **C** and **D,** PC3M tumor-bearing animals were treated orally with NVP-BEZ235 twice daily with a dose of 25 mg/kg for 10 d. Tumor volumes were callipered and body weight was measured during the course of the experiment (**C**). Animals were sacrificed either 1 or 18 h after last dose, and tumor was removed and analyzed as described in **B** (*top*) or sections were analyzed by immunostaining (*bottom*) with an anti-S473P-Akt antibody (**D**). *, $P < 0.05$, one-way ANOVA with Dunnett's *post hoc* test.

Discussion

The prevalence of PI3K signaling abnormalities in human cancer cells has suggested the potential use of PI3K pathway modulators as novel targeted therapeutic agents. Over the past few years, medicinal chemistry activities have been directed to develop pan- or isoform-selective PI3K inhibitors with improved pharmacologic characteristics as well as selectivity profile (41). NVP-BEZ235 is the result of a structure-based design approach from a previously identified dual PDK1/PI3K lead compound. This imidazo-quinoline derivative, which is structurally different from currently available lipid kinase inhibitors

(42–44), exhibits a high degree of inhibitory activity for the four PI3K paralogues. The compound is also active against the most common PI3Kα mutants and mTOR.

Docking studies using a PI3Kα homology model have suggested an intricate network of H-bond interactions involving the PI3Kα paralogue conserved residues Val^{851}, Asp^{933}, and Ser^{774}. These H-bond interactions, together with the potential multiple van der Waals contacts established with conserved hydrophobic residues of the ATP-binding cleft, may account for its potency against PI3K and selectivity profile over protein kinases. Although the interactions with the catalytic site of mTOR was not investigated in detail, systematic docking of the inhibitor in a homology model of mTOR generated as described for PI3Kα (see legend of Fig. 1B) suggests similar binding modes of the compound for these two kinases, particularly with a potential H-bond with the side chain of Ser^{2165} in mTOR (equivalent to Ser^{774} in PI3Kα). Enzyme kinetic analyses showed that NVP-BEZ235 inhibits human PI3Kα competitively with respect to ATP. Cocrystallization studies and single amino acid PI3K mutations are currently ongoing to confirm the preceding molecular modeling predictions.

Compound treatment entailed a decrease in T308P-Akt and S473P-Akt levels as shown by Western blot and ELISA analyses. Using PH domain knock-in mutations, the Akt-mediated PDK1 phosphorylation was shown to be PI3K dependent (45). Several pieces of evidence suggest that the PDK2 activity is primarily due to the mTORC2 complex and that this enzyme has no influence on the phosphorylation of Thr^{308} (4, 46). Hence, inhibition of T308P-Akt levels argues for a direct inhibition of PI3K by

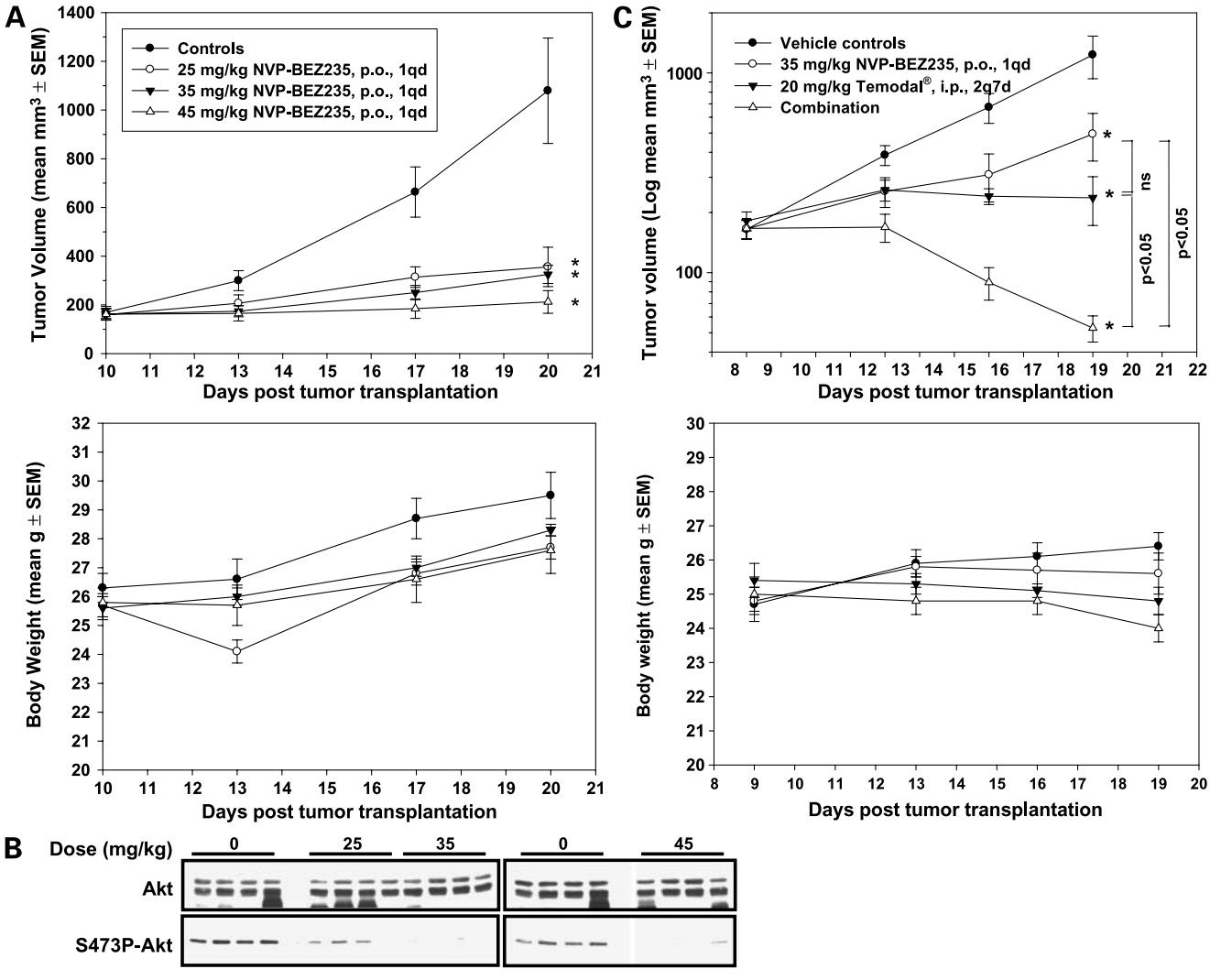

Figure 6. Effects of NVP-BEZ235 against experimental glioblastoma tumor model. U87MG tumor-bearing animals were treated with either NVP-BEZ235 alone (**A**–**C**) or in combination with temozolomide (**C**) at the indicated doses and schedules. Tumor volumes were callipered and body weight was measured during the course of the experiment (**A** and **C**). One hour after last dose, the animals were sacrificed and tumor was removed and analyzed as described in Fig. 5*B* (**B**). *, $P < 0.05$, one-way ANOVA with Dunnett's *post hoc* test.

NVP-BEZ235. However, the lower IC_{50} value obtained for the Ser^{473} levels is unlikely to be due to the sole effect on PI3K but rather to the concomitant blockade of PI3K and mTORC2. Consistent with abrogation of Akt function, decrease in S9P-GSK3β, nuclear localization of FKHRL1, and forkhead-mediated transcription were induced by NVP-BEZ235. The fact that NVP-BEZ235 was more efficient than LY294002 to block Akt activation likely reflects, once more, the synergistic inhibitory effects on PI3K and mTORC2. Systematic analyses of components of different signal transduction pathways (IGF-1, epidermal growth factor, platelet-derived growth factor, interleukin-4, DNA damage, and stress induced) showed that the effects displayed by NVP-BEZ235 are due to selective PI3K/mTOR pathway inhibition, as no inhibitory effects were observed on PI3K independent readouts.

Treatment of U87MG cells with NVP-BEZ235 resulted in a robust growth arrest in the G_1 phase with no apoptosis induction. A similar observation has been reported for other PI3K modulators (43, 44). Although this result might suggest that inhibition of the PI3K pathway per se is not sufficient to drive cells into apoptosis, we cannot exclude that induction of apoptosis could happen with other cell lines or in *in vivo* settings. Hence, when concomitantly challenged with certain cytotoxics or targeted agents, PI3K inhibition would be important to prime the cells to enter programmed cell death. The G_1 arrest observed with NVP-BEZ235 in PC3M seems to be well correlated with the induction of the $p27^{Kip1}$ cyclin-dependent kinase inhibitor. These data are in agreement with the fact that $p27^{Kip1}$ is a target gene for forkhead factors and that NVP-BEZ235 rapidly induces forkhead factor nuclear translocation. Although the effect seems to not require $p21^{Cip1/waf1}$, we cannot exclude that the latter would still be critical in other cell lines.

NVP-BEZ235 displayed a statistically significant antitumor activity against the PTEN-null U87MG and PC3M tumor xenografts. The *in vivo* tumor growth inhibition of NVP-BEZ235 activity was dose dependent, and the observed effect on S473P-Akt levels correlated with the amount of compound present in the tumor tissue. Because mTORC1 complex has been identified as one of the most important downstream effectors of the PI3K-Akt-induced transformation and tumorigenesis (47, 48), it is likely that mTOR inhibition is also contributing to the antitumor activity of the compound. Due to a negative feedback loop involving the phosphorylation of p70S6K, inhibition of mTORC1activity alone could result in the enhanced activation of the PI3K axis (49). Exposure to a dual catalytic PI3K/mTOR inhibitor such as NVP-BEZ235 might therefore be sufficient to avoid PI3K pathway reactivation.

In conclusion, NVP-BEZ235 is a dual pan-PI3K/mTOR inhibitor obtained after an extensive medicinal chemistry effort to modulate the biological activity and pharmaceutical properties of imidazo[4,5-*c*]quinoline-based compounds. NVP-BEZ235 effectively blocks the dysfunctional activation of the PI3K pathway in cellular and *in vivo* settings. The compound displayed diseases stasis in relevant *in vivo* models of human cancer when given orally and enhanced the antitumor activity of other cancer agents. NVP-BEZ235 displays all the features required for clinical development and has entered phase I clinical trials in cancer patients.

Disclosure of Potential Conflicts of Interest

No potential conflicts of interest were disclosed.

Acknowledgments

We thank Marc Hattenberger, Melanie Muller, Fabian Stauffer, Juliane Vaxelaire, Malika, Kazic, Yvonne Ibig-Rehm, and Vincent Unterreiner for excellent technical assistance; Dr. Robert Cozens for critical review of this article; and Dr, David Kwiatkowski for the TSC1/2-null MEF.

References

1. Engelman JA, Luo J, Cantley LC. The evolution of phosphatidylinositol 3-kinases as regulators of growth and metabolism. Nat Rev Genet 2006;7:606–19.

2. Woodgett JR. Recent advances in the protein kinase B signaling pathway. Curr Opin Cell Biol 2005;17:150–7.

3. Sarbassov DD, Guertin DA, Ali SM, Sabatini DM. Phosphorylation and regulation of Akt/PKB by the rictor-mTOR complex. Science 2005;307:1098–101.

4. Guertin DA, Stevens DM, Thoreen CC, et al. Ablation in mice of the mTORC components raptor, rictor, or mLST8 reveals that mTORC2 is required for signaling to Akt-FOXO and PKCα, but not S6K1. Dev Cell 2006;11:859–71.

5. Frias MA, Thoreen CC, Jaffe JD, et al. mSin1 is necessary for Akt/PKB phosphorylation, and its isoforms define three distinct mTORC2s. Curr Biol 2006;16:1865–70.

6. Jacinto E, Facchinetti V, Liu D, et al. SIN1/MIP1 maintains rictor-mTOR complex integrity and regulates Akt phosphorylation and substrate specificity. Cell 2006;127:125–37.

7. Yang Q, Inoki K, Ikenoue T, Guan KL. Identification of Sin1 as an essential TORC2 component required for complex formation and kinase activity. Genes Dev 2006;20:2820–32.

8. Manning BD, Cantley LC. Akt/PKB signaling: navigating downstream. Cell 2007;129:1261–74.

9. Vogelstein B, Kinzler KW. Cancer genes and the pathways they control. Nat Med 2004;10:789–99.

10. Shaw RJ, Cantley LC. Ras, PI(3)K and mTOR signalling controls tumour cell growth. Nature 2006;441:424–30.

11. Samuels Y, Wang Z, Bardelli A, et al. High frequency of mutations of the PIK3CA gene in human cancers. Science 2004;304:554.

12. Kang S, Bader AG, Vogt PK. Phosphatidylinositol 3-kinase mutations identified in human cancer are oncogenic. Proc Natl Acad Sci U S A 2005;102:802–7.

13. Bader AG, Kang S, Vogt PK. Cancer-specific mutations in PIK3CA are oncogenic *in vivo*. Proc Natl Acad U S A 2006;103:1475–9.

14. Zhao JJ, Liu Z, Wang L, Shin E, Loda MF, Roberts TM. The oncogenic properties of mutant p110α and p110β phosphatidylinositol 3-kinases in human mammary epithelial cells. Proc Natl Acad U S A 2005;102:18443–8.

15. Samuels Y, Diaz J, Schmidt-Kittler O, et al. Mutant PIK3CA promotes cell growth and invasion of human cancer cells. Cancer Cell 2005;7:561–73.

16. Cully M, You H, Levine AJ, Mak TW. Beyond PTEN mutations: the PI3K pathway as an integrator of multiple inputs during tumorigenesis. Nat Rev Cancer 2006;6:184–92.

17. Powis G, Bonjouklian R, Berggren MM, et al. Wortmannin, a potent and selective inhibitor of phosphatidylinositol-3-kinase. Cancer Res 1994;54:2419–23.

18. Vlahos CJ, Matter WF, Hui KY, Brown RF. A specific inhibitor of phosphatidylinositol 3-kinase, 2-(4-morpholinyl)-8-phenyl-4H-1-benzopyran-4-one (LY294002). J Biol Chem 1994;269:5241–8.

19. Stein RC. Prospects for phosphoinositide 3-kinase inhibition as a cancer treatment. Endocr Relat Cancer 2001;8:237 – 48.

20. Hu L, Hofmann J, Lu Y, Mills GB, Jaffe RB. Inhibition of phosphatidylinositol 3′-kinase increases efficacy of paclitaxel in *in vitro* and *in vivo* ovarian cancer models. Cancer Res 2002;62:1087 – 92.

21. Bondar VM, Sweeney-Gotsch B, Andreeff M, Mills GB, McConkey DJ. Inhibition of the phosphatidylinositol 3′-kinase-AKT pathway induces apoptosis in pancreatic carcinoma cells *in vitro* and *in vivo*. Mol Cancer Ther 2002;1:989 – 97.

22. Ng SSW, Tsao MS, Nicklee T, Hedley DW. Wortmannin inhibits PKB/Akt phosphorylation and promotes gemcitabine antitumor activity in orthotopic human pancreatic cancer xenografts in immunodeficient mice. Clin Cancer Res 2001;7:3269 – 75.

23. Stauffer F, Maira S-M, Furet P, Garcia-Echeverria C. Imidazo[4,5-*c*]quinolines as inhibitors of the PI3K/PKB-pathway. Bioorg Med Chem Lett 2008;18:1027 – 30.

24. Garcia-Echeverria C, Pearson MA, Marti A, et al. *In vivo* antitumor activity of NVP-AEW541-A novel, potent, and selective inhibitor of the IGF-IR kinase. Cancer Cell 2004;5:231 – 9.

25. Walker EH, Pacold ME, Perisic O, et al. Structural determinants of phosphoinositide 3-kinase inhibition by wortmannin, LY294002, quercetin, myricetin, and staurosporine. Mol Cell 2000;6:909 – 19.

26. Koresawa M, Okabe T. High-throughput screening with quantitation of ATP consumption: a universal non-radioisotope, homogeneous assay for protein kinase. Assay Drug Dev Technol 2004;2:153 – 60.

27. Walker EH, Perisic O, Ried C, Stephens L, Williams RL. Structural insights into phosphoinositide 3-kinase catalysis and signalling. Nature 1999;402:313 – 20.

28. Huang CH, Mandelker D, Schmidt-Kittler O, et al. The structure of a human p110α/p85α complex elucidates the effects of oncogenic PI3Kα mutations. Science 2007;318:1744 – 8.

29. Davis RJ. Signal transduction by the JNK group of MAP kinases. Cell 2000;103:239 – 52.

30. Bakkenist CJ, Kastan MB. DNA damage activates ATM through intermolecular autophosphorylation and dimer dissociation. Nature 2003; 421:499 – 506.

31. Kurz EU, Lees-Miller SP. DNA damage-induced activation of ATM and ATM-dependent signaling pathways. DNA Rep 2004;3:889 – 900.

32. Hawkins PT, Anderson KE, Davidson K, Stephens LR. Signalling through Class I PI3Ks in mammalian cells. Biochem Soc Trans 2006;34: 647 – 62.

33. Burgering BM, Medema RH. Decisions on life and death: FOXO forkhead transcription factors are in command when PKB/Akt is off duty. J Leuk Biol 2003;73:689 – 701.

34. Xuan Z, Zhang MQ. From worm to human: bioinformatics approaches to identify FOXO target genes. Mech Ageing Dev 2005;126:209 – 15.

35. Tee AR, Anjum R, Blenis J. Inactivation of the tuberous sclerosis complex-1 and -2 gene products occurs by phosphoinositide 3-kinase/Akt-dependent and -independent phosphorylation of tuberin. J Biol Chem 2003;278:37288 – 96.

36. Tee AR, Fingar DC, Manning BD, Kwiatkowski DJ, Cantley LC, Blenis J. Tuberous sclerosis complex-1 and -2 gene products function together to inhibit mammalian target of rapamycin (mTOR)-mediated downstream signaling. Proc Natl Acad U S A 2002;99:13571 – 6.

37. Mellinghoff IK, Wang MY, Vivanco I, et al. Molecular determinants of the response of glioblastomas to EGFR kinase inhibitors. N Engl J Med 2005;353:2012 – 24.

38. Jiang BH, Zheng JZ, Aoki M, Vogt PK. Phosphatidylinositol 3-kinase signaling mediates angiogenesis and expression of vascular endothelial growth factor in endothelial cells. Proc Natl Acad U S A 2000;97:1749 – 53.

39. Mason WP, Cairncross JG. Drug Insight: temozolomide as a treatment for malignant glioma—impact of a recent trial. Nat Clin Pract Neurol 2005; 1:88 – 95.

40. Hirose Y, Katayama M, Mirzoeva OK, Berger MS, Pieper RO. Akt activation suppresses Chk2-mediated, methylating agent-induced G2 arrest and protects from temozolomide-induced mitotic catastrophe and cellular senescence. Cancer Res 2005;65:4861 – 9.

41. Maira SM, Voliva C, Garcia-Echeverria C. Class IA phosphatidylinositol 3-kinase: from their biologic implication in human cancers to drug discovery. Exp Opin Ther Targets 2008;12:223 – 38.

42. Knight ZA, Shokat KM. Chemically targeting the PI3K family. Biochem Soc Trans 2007;35:245 – 49.

43. Fan QW, Knight ZA, Goldenberg DD, et al. A dual PI3 kinase/mTOR inhibitor reveals emergent efficacy in glioma. Cancer Cell 2006;9:341 – 9.

44. Yaguchi S, Fukui Y, Koshimizu I, et al. Antitumor activity of ZSTK474, a new phosphatidylinositol 3-kinase inhibitor. J Natl Cancer Inst 2006;98:545 – 56.

45. McManus EJ, Collins BJ, Ashby PR, et al. The *in vivo* role of PtdIns(3,4,5)P3 binding to PDK1 PH domain defined by knocking mutation. EMBO J 2004;23:2071 – 82.

46. Shiota C, Woo JT, Lindner J, Shelton KD, Magnuson MA. Multiallelic disruption of the rictor gene in mice reveals that mTOR complex 2 is essential for fetal growth and viability. Dev Cell 2006;11:583 – 9.

47. Skeen JE, Bhaskar PT, Chen CC, et al. Akt deficiency impairs normal cell proliferation and suppresses oncogenesis in a p53-independent and mTORC1-dependent manner. Cancer Cell 2006;10:269 – 80.

48. Neshat MS, Mellinghoff IK, Tran C, et al. Enhanced sensitivity of PTEN-deficient tumors to inhibition of FRAP/mTOR. Proc Natl Acad U S A 2001;98:10314 – 9.

49. O'Reilly KE, Rojo F, She QB, et al. mTOR inhibition induces upstream receptor tyrosine kinase signaling and activates Akt. Cancer Res 2006;66: 1500 – 8.